Charge distributions of medium energy He ions scattered from metal surfaces

Kei Mitsuhara, Akihiro Mizutani and Masaru Takizawa

Department of Physical Sciences, Factory of Science and Engineering, Ritsumeikan University, Kusatu, Shiga 525-8577, Japan

Abstract

He^+ fractions for medium energy He ions emerging from clean Cu(001) and Ag(001) surfaces has been studied extensively using a toroidal electrostatic analyzer with an excellent energy resolution. He^+ fractions for medium energy He ions scattered from top-layer atoms of both the surfaces were equilibrated at emerging angles above ~75° and increase with increasing emerging energy. Emerging angle and energy dependence of He^+ fractions for that were indicated the same tendency together. Copper and silver are homologous elements. Thus it suggests that the same interaction has caused because the electronic state is also similar.

1. Introduction

High-resolution medium energy ion scattering (MEIS) has been developed as a powerful tool to investigate the structures of solid surfaces and elemental depth profiles [1-6]. One of the advantages of MEIS analysis is that it's possible to decide about the absolute quantity of the element. For precise spectrum analysis, it is important to know reliable stopping power and energy straggling values and line shape as well as charge fractions of emerging He ions. The stopping values have been compiled as a database in a semi-empirical manner by Ziegler and co-workers [7]. We employed the Lindhard-Scharff formula [8] which gives energy straggling values. The spectrum for He ions scattered from near-surface atoms has an asymmetric line shape because of excitations of inner shell electrons by a large-angle collision. This asymmetric line shape can be well approximated by an exponentially modified Gaussian (EMG) distribution function [9, 10]. In most of MEIS analysis, a magnetic or electrostatic analyzer is usually used. Therefore, it is indispensable to have reliable charge fraction data for H and He ions. In the case of He ions, the He^+ fraction depends on emerging energy and angle as well as surface atomic species [11-14].

In this study, we measured the He^+ fractions for 30-140 keV He^+ ions incident on Cu(001) and Ag(001) and scattered from the top-layer atoms. As the results, it was found that the He^+ fractions depend strongly on emerging energy and angle. Interestingly, both He^+ fractions were indicated the same tendency together. It suggests that the same interaction has caused because the electronic state is also similar.

2. Experiments and spectrum analysis

The experiment was performed at beamline 8 named SORIS set up at Ritsumeikan SR Center [15]. A duo-plasma ion source provided He^+ ions with a good emittance, which were accelerated from 5 up to 200 keV and finally collimated to a beam size of 0.18 and 2.0 mm in horizontal and vertical planes, respectively. Samples were mounted on a six-axis goniometer in an ultrahigh vacuum (UHV) chamber ($\leq 2\times10^{-8}$ pa). In order to suppress secondary electron emission, the sample was biased by +90 V to ground. Scattered He^+ ions were energy-analyzed with a toroidal electrostatic analyzer (ESA). A three-stage micro-channel plate combined with a position sensitive detector gives an excellent energy resolution of $\Delta E/E \cong 1\times10^{-3}$ (FWHM) [16]. The detection

efficiency (ε) and the solid angle ($\Delta\Omega$) subtended by the toroidal ESA detector were $\varepsilon = 0.44$ and $\Delta\Omega = 7.64\times10^{-5}$ [str], respectively. In order to avoid radiation damage of the sample surface, we shifted the beam position on the sample surface after accumulating a beam current of 1 μC.

We purchased Cu(001) and Ag(001) substrates whose surfaces were mirror finished. The substrates were prepared by several cycles of 1.0-1.5 keV Ar^+ sputtering and annealing at 870 K for 30 min in UHV. The surface showed a clear (1×1) pattern, which was observed by reflection high energy electron diffraction (RHEED). All the experiments were performed *in situ* under UHV conditions ($\leq 2\times10^{-8}$ Pa).

The yield of He^+ ions scattered from the n-th layer atoms, Y_n is expressed by

$$Y_n\left(E_{out}(n)\right) = Q(d\sigma/d\Omega)N\Delta x\Delta\Omega\varepsilon\eta^+P_{CL}(n)/cos\theta_{in} \quad (1)$$

where $E_{out}(n)$ is the emerging energy of He^+ ions scattered from the n-th layer atoms, which is loss during emerging from the n-th layer atoms. Q is number of incident He^+ ions, $d\sigma/d\Omega$ is differential scattering cross section, $N\Delta x$ is number of target atoms [atoms/cm^2] and η^+ is He^+ fraction. The close encounter probability for the n-th layer atoms is denoted by $P_{CL}(n)$ and θ_{in} is an incident angle with respect to surface normal. We employed the scattering cross sections proposed by LEE and Hart [17]. The close encounter probability, $P_{CL}(n)$ for the atoms in each layer was calculated by the Monte Carlo (MC) simulations of He ion trajectories based on the single-row approximation. The root-mean-square (rms) one-dimensional bulk thermal vibration amplitudes for Cu and Ag atoms were calculated based on the Debye approximation. It was also assumed that the thermal vibration amplitudes for the top layer atoms in the surface normal direction were enhanced by $\sqrt{2}$ compared with that of bulk. When we determine the fractions of the He^+ ions precisely, we need to determine the yield of He^+ ions scattered from each layer atoms. Now therefore, it is essentials to fit precisely the observed spectrum. As mention before, we used the asymmetric line shape expressed by EMG function [9, 10], which is given by

$$f(E-E_{out}(n)) = \frac{1}{2\sigma_0}\exp[-\frac{1}{2\sigma_0}\{2(E-E_{out}(n))-\frac{\sigma_n^2}{\sigma_0}\}]\cdot\{1+erf(\frac{E-E_{out}(n)-\sigma_n^2/\sigma_0}{\sqrt{2}\sigma_n})\} \quad (2)$$

where $erf(x)$ is an error function, σ_n is the energy spread of emerging He^+ ions backscattered from the n-th layer atoms and σ_0 is an asymmetric parameter calculated by the Casp-version 5[18]. Via the above procedure, the MEIS spectrum for He^+ ions scattered from each layer atoms was uniquely synthesized. In such a way, we can determine the He^+ fraction (η^+) as well as stopping power

values by best-fitting the simulated spectrum to observed one.

3. Results and discussions

Figure 1(a) and (b), respectively show the MEIS spectra for 122.67 keV and 116.40 keV He^+ ions incident along the [110]-axis and scattered to the $[1\bar{1}0]$-axis (45°) from Cu(001) and Ag(001). Best-fits were obtained assuming the stopping power value of 1.7 and 1.8 times the Ziegler's data and η^+= 0.55 and 0.53, respectively. Here, we used the asymmetric parameters σ_0 values of 130 and 160 eV, respectively for 122 keV and 116 keV He^+ impact on Cu and Ag given by CasP version 5.2 [18].

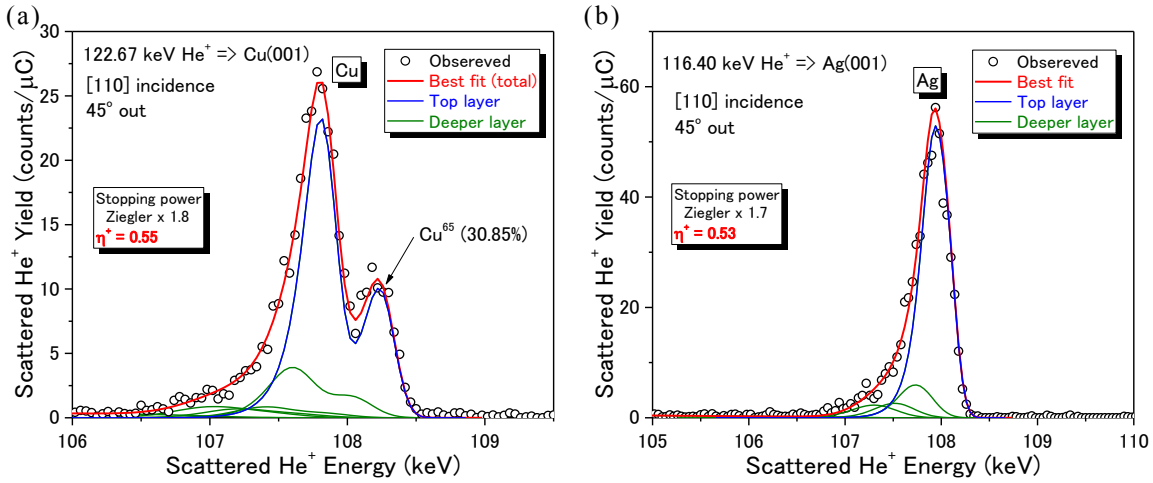

Fig. 1 (a) MEIS spectrum observed for 122.6 keV He^+ ions incident along [110]-axis and scattered Cu(001) to 45° with respect to surface normal. Red curve (thick) indicates best-fitted spectrum and blue and green curves (thin) denote scattering component from top-layer Cu and those from deeper layer Cu, respectively. (b) MEIS spectrum observed for 116.4 keV He^+ ions incident along [110]-axis and scattered from Ag(001) to 45°.

Thus, we measured the emerging-angle dependent He^+ fractions for scattering component from the top layer atoms of Cu(001) and Ag(001), as shown in Fig. 2. Here, the emerging energy is fixed to 108 keV. The He^+ fractions for Cu(001) and Ag(001) are decreased slowly with increasing emerging angle and saturated above 75°. The saturated He^+ fractions are smaller than the Marion-Young's data [19]. Interestingly, the both angle dependence of He^+ fraction is almost the same tendency.

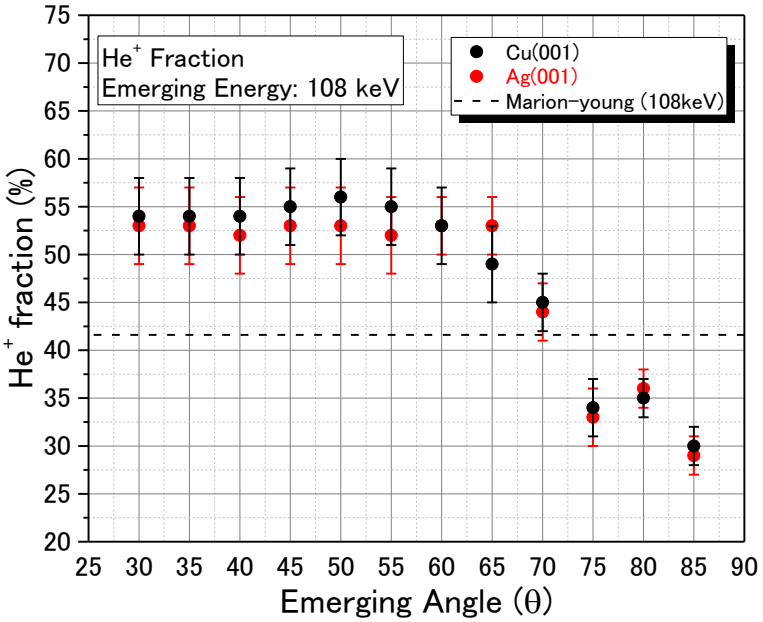

Fig. 2 He^+ fractions determined for Cu(001) (full black circles) and Ag(001) (full red circles) as a function of emerging angles. Emerging energy was fixed to 108 keV. Dash line (black) denotes the equilibrium He^+ fraction given by Marion and Young [19].

Next, we measured dependence of He^+ fractions upon emerging energy for the scattering component from top atoms at Cu(001) and Ag(001) (Fig. 3). Here, we fixed an emerging angle to 80°. The both He^+ fractions considerably smaller than the Marion-Young's data [19] under 100 keV. On the other hand, the He^+ fractions are close to that data above 100 keV. It is also found that the both angle dependence of He^+ fractions is the same tendency.

He ion immediately after a large angle collision has no bound electron because of the energy-time uncertainty. The collision time defined as the time lapse during a strong deflection of the trajectory in the large-angle collision is estimated roughly to be of the order of 10^{-17} sec, which results in an energy uncertainty of 100 – 200 eV exceeding the binding energy (54 eV) of the 1s electron of H^+ ion. The scattered He^{2+} ion experiences electron capture and loss processes, mainly the capture process before escaping from the surface. Copper and silver are homologous elements. Thus it suggests that the same interaction has caused because the electronic state is also similar. For large emerging angle, the charge state becomes equilibrium due to a long enough path length in the interacting region. According to the jellium model (homogeneous electron gas) [20], an electronic surface is expanded about a half monolayer from the top

atomic plane toward the vacuum side. In the present energy region from 50 to 130 keV, primary charge states are He^0 (neutral) and He^+ and the fraction of He^{2+} is negligibly small less than 5 %[19].

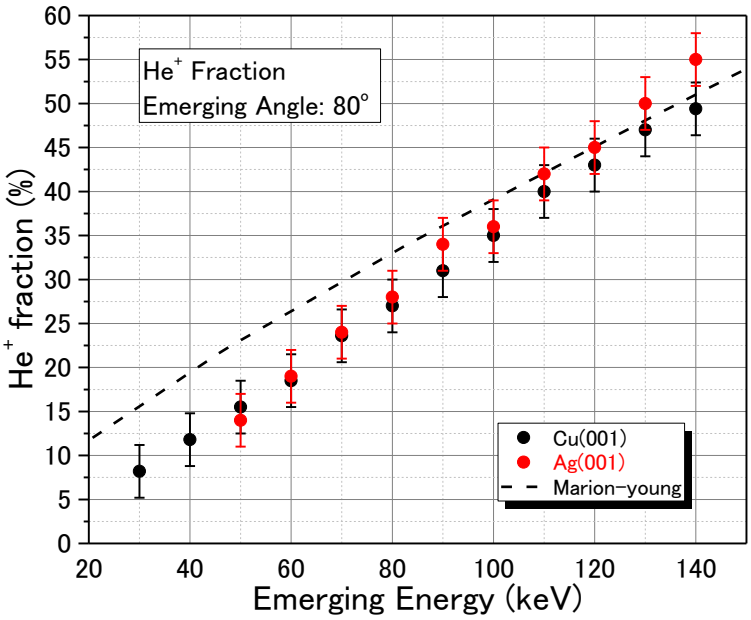

Fig. 3 He^+ fractions determined for Cu(001) (full black circles) and Ag(001) (full red circles) as a function of emerging energy. Emerging angle was fixed to 108 keV. Dash line (black) denotes the equilibrium He^+ fraction given by Marion and Young [19].

4. Conclusions

In this study, we measured He^+ fractions scattered from top layer atoms of Cu(001) and Ag(001). For both emerging energy and emerging angle dependence, He^+ fractions at Cu(001) and Ag(001) were indicated the same tendency together**.** The reason of the same distribution of He^+ fraction is attribution to the fact that copper and silver are homologous elements. Thus it suggests that the same interaction has caused because the electronic state is also similar. A quantitative discussion is possible to calculate electron capture and loss cross sections for He^+ and He^{2+} involving precise surface arrangement and electronic state.

Acknowledgement

The authors would like to appreciate T. Aoki for his help in carrying out the

MEIS experiments.

References

[1] J.F. van der Veen, Surf. Sci. Rep. **5** (1985) 199.

[2] J. Vrijmoeth, P.M. Zagwijn, J.W.M. Frenken, J.F. van der Veen, Phys. Rev. Lett. **67** (1991) 1134.

[3] K. Kimura, K. Nakajima, Y. Fujii, M. Mannami, Surf. Sci. **318** (1994) 363.

[4] P. Statiris, H.C. Lu, T. Gustafsson, Phys. Rev. Lett. **72** (1994) 3574.

[5] T. Nishimura, A. Ikeda, H. Namba and Y. Kido, Surf. Sci. **411** (1998) L834.

[6] P. Bailey, T.C.Q. Noakes, D.P. Woodruff, Surf. Sci. **426** (1999) 358.

[7] J.F. Ziegler, J.P. Biersack and U.L. Littmark, *The Stopping and Range of Ions in Solids*, (Pergamon Press, New York, 1985).

[8] J. Lindhard and M. Scharff, K. Dan. Vidensk. Selsk. Mat. Fys. Medd. **27** (1953) 1.

[9] P. L. Grande, A. Hentz, R. P. Pezzi, I. J. R. Baumvol and G. Schiwietz, Nucl. Instrum. and Method B **256** (2007) 92.

[10] M. Hazama, Y. kitsudo, T. Nishimura, Y. Hoshino, P. L. Grande, G. Schiwietz and Y. Kido, Phys. Rev. B **78**(2008)193402.

[11] Y. Kido, T. Nishimura and F. Fukumura, Phys. Rev. Lett. **82** (1999) 3352.

[12] T. Okazawa, K. Shibuya, T. Nishimura and Y. Kido, Nucl. Instrum. Methods B **256** (2007) 1.

[13] Y. Kitsudo, K. Shibuya, T. Nishimura, Y. Hoshino, I. Vickridge and Y. Kido, Nucl. Instrum. Methods B **267** (2009) 566.

[14] K. Mitsuhara, T. Kushida, H. Okumura, H. Matsumoto, A. Visikovskiy, Y. Kido, Surf. Sci. **604** (2010) L48.

[15] Y. Kido, H. Namba, T. Nishimura, A. Ikeda, Y. Yan and A. Yagishita, Nucl. Instrum. Methods B **136-138** (1998) 798.

[16] Y. Kido, T. Nishimura, Y. Hoshino and H. Namba, Nucl. Instr. and Meth. B **161–163** (2000) 371.

[17] S.R. Lee and R.R. Hart, Nucl. Instrum. Methods B **79** (1993) 463.

[18] http://www.helmholtz-berlin.de/people/gregor-schiwietz/casp_en.html.

[19] J.B. Marion and F. C. Young, *Nuclear Reaction Analysis - Graphs and Tables* (North Holland, Amsterdam, 1968).

[20] N.D. Lang and W. Kohn, Phys. Rev. B **3** (1970) 1215.